

# High-sensitivity fiber-tip pressure sensor with graphene diaphragm

Jun Ma,<sup>1</sup> Wei Jin,<sup>1,\*</sup> Hoi Lut Ho,<sup>1</sup> and Ji Yan Dai<sup>2</sup>

<sup>1</sup>Department of Electrical Engineering, The Hong Kong Polytechnic University, Hung Hom, Kowloon, China

<sup>2</sup>Department of Applied Physics, The Hong Kong Polytechnic University, Hung Hom, Kowloon, China

\*Corresponding author: eewjin@polyu.edu.hk

Received April 10, 2012; revised April 23, 2012; accepted April 23, 2012;

posted April 24, 2012 (Doc. ID 166456); published June 20, 2012

A miniature fiber-tip pressure sensor was built by using an extremely thin graphene film as the diaphragm. The graphene also acts as a light reflector, which, in conjunction with the reflection at the fiber end–air interface, forms a low finesse Fabry–Perot interferometer. The graphene based sensor demonstrated pressure sensitivity over 39.4 nm/kPa with a diaphragm diameter of 25  $\mu\text{m}$ . The use of graphene as diaphragm material would allow highly sensitive and compact fiber-tip sensors. © 2012 Optical Society of America

OCIS codes: 060.2370, 120.2230.

Fabry–Perot interferometers (FPIs) built at the tips of optical fiber have been studied for the detection of pressure and acoustic waves in remote, space limited, and harsh environment [1–3]. Among key elements that determine the pressure sensitivity of the FPI are the properties of the diaphragm. The pressure sensitivity, which is defined as the ratio of the center deflection of the diaphragm to the pressure difference, can be improved by the use of a larger and thinner diaphragm. To produce miniature sensors, the diaphragm diameter is limited and the most effective method to improve the pressure sensitivity is to reduce the thickness of the diaphragm. Zhu *et al.* reported a fiber-tip pressure sensor made by splicing a 66  $\mu\text{m}$  diameter and 1.88  $\mu\text{m}$  thick silica diaphragm to a microcavity at an optical fiber end, and demonstrated a pressure sensitivity of 1.49 nm/psi (1 psi = 6.89 kPa) [1]. By further reducing the thickness through online hydrofluoric acid (HF) etching, Donlagic and Cibula demonstrated a fiber-tip sensor with a 62.5  $\mu\text{m}$  diameter diaphragm and obtained a pressure sensitivity of 3.4 nm/kPa [2]. Wang *et al.* reported a fiber-tip pressure sensor with a 65  $\mu\text{m}$  diameter and 0.75  $\mu\text{m}$  thick silica diaphragm and achieved a pressure sensitivity of 11 nm/kPa [3]. Recently, Xu *et al.* reported a fiber-tip FPI made with a 125  $\mu\text{m}$  diameter and 130 nm thick silver diaphragm and demonstrated a pressure sensitivity of 70.5 nm/kPa [4].

In this Letter, we report the construction of a fiber-tip FPI sensor with graphene as the sensitive diaphragm. Graphene is the thinnest film in the universe, and the thickness of a single layer of graphene is  $\sim 0.335$  nm [5]. Graphene has very high mechanical strength and can be stretched by as much as 20% [6]. With such a novel material, it is possible to build miniature pressure and acoustic sensors with high sensitivity and dynamic range.

Figure 1 shows the microscope images of a fiber-tip FPI sensor. A standard single mode fiber was first fusion-spliced to a pure silica capillary (inner diameter 25  $\mu\text{m}$ ) with the same outer diameter. An Ericsson FSU-975 fusion splicer was used, and the fusion current and the fusion time of the three-step procedure of the splicer were set as follows: 10 mA/0.2 s, 11.5 mA/0.2 s, and 10.6 mA/0.4 s. The capillary is then cut, with the aid of a microscope, at a distance of a few tens of micrometers from the splice joint. An open air cavity

at the fiber tip is then constructed, as shown in Figs. 1(a) and 1(b). The open cavity was then sealed by a thin graphene film [Fig. 1(c)], which acts as a diaphragm and deflects with external pressure variation. The process for preparing the graphene film and transferring it onto the fiber tip to form a sealed microcavity is shown in Fig. 2. We started with a commercial graphene/Ni/SiO<sub>2</sub>/Si sample in which a few-layer graphene film was grown, by chemical vapor deposition (CVD), on a Nickel (Ni) film deposited on a SiO<sub>2</sub>/Si substrate (Graphene-supermarket.com). To separate the graphene film from the substrate, the sample was immersed into a FeCl<sub>3</sub> solution with a concentration of 0.05 g/mL [Figs. 2(a) and 2(d)] to etch away the Ni layer. Just before the Ni layer was completely etched off, which corresponds to the detachment of the graphene film from the SiO<sub>2</sub>/Si substrate, the sample was transferred to de-ionized (DI) water. After suspension on DI water for  $\sim 12$  h to remove the residual Fe and Ni ions, the sample was dipped into clean DI water with a floating-off process to delaminate the graphene from the SiO<sub>2</sub>/Si substrate [7], and the graphene film would then float on the water surface [Fig. 2(e)]. The next step was to transfer the graphene film onto the surface of the fiber-tip air cavity. The fiber tip with the open air cavity [Fig. 1(a)] was inserted into a ferrule with an inner diameter of 127  $\mu\text{m}$ , and its endface was adjusted to be in the same plane with the endface of the ferrule. The ferrule–fiber-tip assembly was then moved down slowly toward the floating graphene as shown in Fig. 2(b), until it touched the graphene sample. The graphene together with a water layer was then attached to the surface of the assembly. The assembly was then left to dry at room

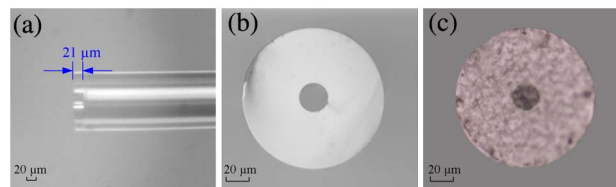


Fig. 1. (Color online) Microscope images of (a) fiber-capillary tip, (b) cross section of the tip endface, (c) the graphene film-covered fiber-capillary tip.

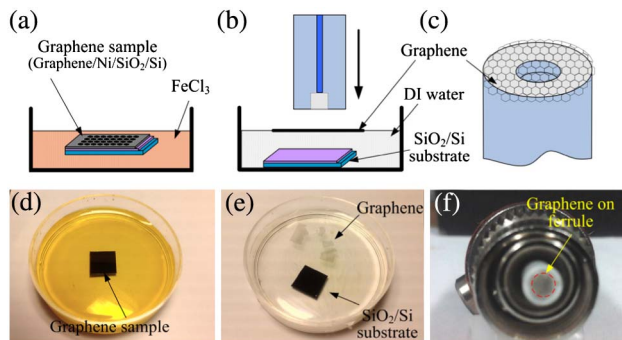


Fig. 2. (Color online) Fabrication process of the fiber-tip microcavity with a graphene diaphragm. (a) Etching off the Ni layer by immersing the sample into a  $\text{FeCl}_3$  solution; (b) transferring the graphene film floating on the water surface to the surface of the fiber-tip open cavity, (c) schematic showing the graphene film covering the fiber-tip microcavity; photographs of (d) graphene/Ni/SiO<sub>2</sub>/Si sample floating on  $\text{FeCl}_3$  solution, (e) graphene film floating on DI water, (f) graphene film on the surface of the ferrule-fiber-tip microcavity assembly.

temperature in a cabinet for about half an hour. During the drying process, we found that water was drawn, by capillary force, into the space between the fiber and the ferrule. This might have helped to avoid damaging the graphene film under the water surface tension and preventing the sealing of water into the microcavity. After water evaporation, the graphene is firmly stuck to the surface of the fiber-tip by the van der Waals interaction to form a sealed microcavity [8], as illustrated in Figs. 2(c) and 2(f). The microscope image of a sealed fiber-tip microcavity is shown in Fig. 1(c).

The microcavity was characterized by using a reflective system similar to that described in [9]. A broadband source comprising five light emitting diodes (LEDs) with a central wavelength from 1200 to 1700 nm was used to illuminate the microcavity, and the reflection spectrum was analyzed by an optical spectrum analyzer (OSA) (0.01 nm resolution) through the use of an optical circulator. Figure 3(a) shows a typical reflection spectrum. Considering the small reflectivity of the silica-air interface as well as the graphene film [9,10], higher-order reflections from these surfaces may be ignored and the periodic reflection spectrum in Fig. 3(a) may be regarded as a result of two-beam interference. The length of the air cavity  $d$  can then be calculated by  $d = \lambda^2/2\delta\lambda$ , where  $\lambda$  and  $\delta\lambda$  are respectively the dip (or peak) wavelength

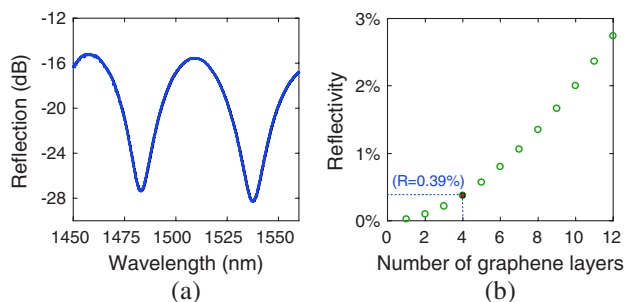


Fig. 3. (Color online) (a) Measured reflection spectrum of the FPI, (b) calculated reflectance as a function of the number of graphene layers. The complex refractive index used in the calculation is  $3.45 - j2.32$  for graphene at 1550 nm [11].

and the wavelength spacing between the two fringes. From Fig. 3(a), the cavity length  $d$  is determined to be 21  $\mu\text{m}$ , in agreement with the value measured by the microscope [Fig. 1(a)].

The reflectivity of the two cavity surfaces was examined in detail. Before the graphene film placement, the reflectivity of the fiber end silica-air interface was first measured with a power meter to be 1.3%–2.0%, depending on samples. These values are smaller than the Fresnel coefficient calculated for a perfect silica-air interface at normal incidence ( $\sim 3.4\%$  at  $\sim 1550$  nm), possibly due to imperfect (tilted) fiber cleaving. The reflectivity of graphene film was determined, by the curve fit to the measured reflection spectrum [e. g., Fig. 3(a)], to be 0.27%–0.79%. These results were verified by measurement with an optical low coherence reflectometer (OLCR). The reflectivity of the graphene film with an increasing number of graphene layers was also calculated, and the results are shown in Fig. 3(b). According to the product datasheet, the graphene film grown on nickel is not uniform, and its thickness varies from 1 to 4 layers. From Fig. 3(b), the reflectivity of the graphene film should be less than 1%, in agreement with the experimentally measured values.

The pressure response of the sensor was tested with the same setup but the sensor head was placed in a sealed pressure chamber. The wavelength shift  $\Delta\lambda$  of the interference fringe under different pressures was measured, and the cavity length change  $\Delta d$ , which equals the diaphragm deflection  $\Delta\delta$ , was calculated by using the relationship  $\Delta d = d \cdot \Delta\lambda/\lambda$  [9]. The cavity length is found to decrease with the increase of the external pressure, following a nonlinear curve as shown in Fig. 4(a). This is expected since the linear model is only applicable for a deflection smaller than 30% of the thickness of the diaphragm [12]. The average pressure sensitivity over the range from 0 to 5 kPa is estimated to be 39.4 nm/kPa. The relationship between the deflection  $\delta$  of a circular diaphragm made of a linear isotropic elastic material and the pressure change  $P$  may be described by [6,13]

$$P = \frac{2Et}{(1-\nu)a^4}\delta^3 + \frac{4\sigma_0 t}{a^2}\delta \quad (1)$$

where  $E$  is the Young's modulus of the graphene ( $\sim 1$  Tpa),  $\nu$  is its Poisson's ratio ( $\sim 0.17$ ) [6],  $\sigma_0$  is the graphene film pre-stress, and  $a$  and  $t$  are respectively the radius and the thickness of the graphene film. Through curve fitting of the experimental data in Fig. 4(a), the pre-stress is found to be 1.2 GPa, and the thickness of the graphene

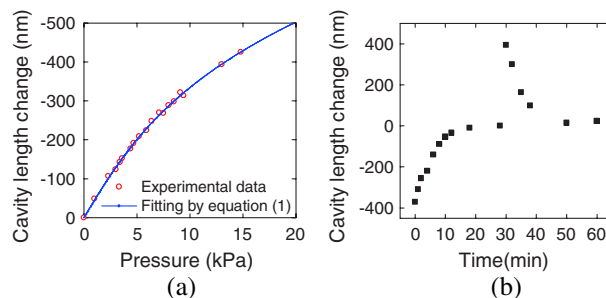


Fig. 4. (Color online) (a) Pressure response of the fiber-tip micro-cavity sensor, (b) cavity length change versus time for an initially applied pressure of  $\sim 13$  kPa.

film  $\sim 0.71$  nm, corresponding to a 2-layer graphene. This value of pre-stress is within the range measured by use of an atomic force microscope (AFM) tip, which indicates a broad range of pre-stresses varying from 0.2 to 2.2 GPa due to the stretching of the graphene caused by the van der Waals attraction to the cavity inner wall [6].

It should be mentioned that during pressure tests, the graphene sealed cavity was found slightly leaky. Figure 4(b) shows the measured cavity length change as a function of time  $T$  when a pressure of  $\sim 13$  kPa is applied at  $T \sim 0$  and released (chamber opened) at  $T \sim 30$  min. The graphene diaphragm deflects inward initially because the external pressure is higher than that inside the microcavity, and the deflection gradually reduces and returns to initial state (zero deflection), which indicates that the cavity is leaking. The time to achieve pressure equilibrium is about 20 min. When the applied pressure is released, the graphene diaphragm deflects in the opposite direction instantly, and the deflection reduces gradually and returns to equilibrium again after  $\sim 20$  min. As reported in [14], the graphene itself is impermeable to all standard gases, and the leakiness might be attributed to the nonideal adhesion of the graphene layer to the silica capillary endface, which is affected by the surface roughness of the capillary end. Due to this leakiness problem, continuous tests of the sensor under static pressure would cause measurement errors. Hence, our measurement of the pressure response was conducted by applying a target pressure, recording the spectrum, and releasing the pressure, with all these steps done within the duration of only several seconds. By repeating this process with different applied pressures, the pressure response shown in Fig. 4(a) was obtained. We also carried out tests for pressure up to 100 kPa, but the interference fringes were found to shift quickly due to the leakiness of the cavity, which prohibited accurate determination of the applied pressure. As demonstrated in [8], the graphene could withstand pressure up to 2.5 MPa, indicating the graphene-based fiber-tip sensors could operate over a large dynamic range. Tight sealing of the cavity by smoothing out the capillary endface and additional adhesion or bonding is a future possibility.

Several fiber-tip microcavities were constructed and found to have different pressure sensitivities ranging from 36 to 63 nm/kPa over a pressure range of 0–5 kPa. According to Eq. (1), the pressure sensitivity depends on the pre-stress and the thickness of the graphene film. By least-square curve fitting of the pressure response curves, the pre-stress and the thickness of the graphene samples were obtained for different fiber-tip microcavities, and they are shown in Fig. 5. The pre-stress ranges from 1 to 2.1 GPa, within the previously reported range [6]. The pre-stress is not yet under control with our current fabrication setup. The graphene thickness ranges from 0.26 to 0.76 nm, corresponding to 1 to 2 graphene layers.

Compared with previously reported fiber-tip pressure sensors, the sensor presented here used a much smaller diaphragm (and thus potentially smaller size sensor head) and has achieved a high sensitivity. Taking the sensor reported in [4] as an example, a pressure sensitivity of 70.5 nm/kPa was achieved with a 125  $\mu\text{m}$  diameter and 130 nm thick diaphragm. According to the linear sensitivity formula in [1], if the diaphragm diameter is

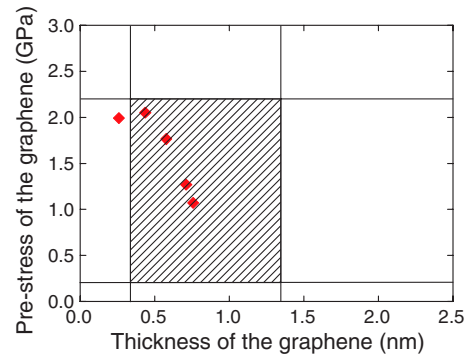


Fig. 5. (Color online) Fitted initial surface pre-stress and graphene film thickness from the measured pressure response of several fiber-tip microcavity sensors.

reduced to 25  $\mu\text{m}$ , the sensitivity of the sensor would be reduced by 625 times to 0.11 nm/kPa, which is more than 300 times smaller than the sensitivity we have achieved. The sensor performance could be further improved by using a larger graphene diaphragm with a better quality (e.g., using graphene from mechanical exfoliation), and better graphene transferring method. The small size and high sensitivity of the graphene-based fiber-tip sensors would find applications in miniature and highly sensitive pressure, acoustic, and mass sensors [15] for biomedical, environmental, microsystem, and nanosystem applications.

The authors thank the Hong Kong SAR government for support through GRF grant PolyU 5196/09E, and Hong Kong PolyU through grant J-BB9K and a studentship.

## References

1. Y. Zhu, K. L. Cooper, G. R. Pickrell, and A. Wang, *J. Lightwave Technol.* **24**, 861 (2006).
2. D. Donlagic and E. Cibula, *Opt. Lett.* **30**, 2071 (2005).
3. W. Wang, N. Wu, Y. Tian, C. Niezrecki, and X. Wang, *Opt. Express* **18**, 9006 (2010).
4. F. Xu, D. Ren, X. Shi, C. Li, W. Lu, L. Lu, L. Lu, and B. Yu, *Opt. Lett.* **37**, 133 (2012).
5. K. S. Novoselov, A. K. Geim, S. V. Morozov, D. Jiang, Y. Zhang, S. V. Dubonos, I. V. Gregorieva, and A. A. Firsov, *Science* **306**, 666 (2004).
6. C. Lee, X. Wei, J. W. Kysar, and J. Hone, *Science* **321**, 385 (2008).
7. Q. Bao, H. Zhang, Y. Wang, Z. Ni, Y. Yan, Z. X. Shen, K. P. Loh, and D. Y. Tang, *Adv. Funct. Mater.* **19**, 3077 (2009).
8. S. P. Koenig, N. G. Boddeti, M. L. Dunn, and J. S. Bunch, *Nat. Nanotech.* **6**, 543 (2011).
9. J. Ma, J. Ju, L. Jin, and W. Jin, *IEEE Photon. Technol. Lett.* **23**, 1561 (2011).
10. H. S. Skulason, P. E. Gaskell, and T. Szkopek, *Nanotechnology* **21**, 295709 (2010).
11. F. J. Nelson, V. K. Kamineni, T. Zhang, E. S. Comfort, J. U. Lee, and A. C. Diebold, *Appl. Phys. Lett.* **97**, 253110 (2010).
12. M. D. Giovanni, *Flat and Corrugated Diaphragm Design Handbook* (Marcel Dekker, 1982).
13. C. Lee, X. Wei, Q. Li, R. Carpick, J. W. Kysar, and J. Hone, *Phys. Stat. Sol. B* **246**, 2562 (2009).
14. J. S. Bunch, S. S. Verbridge, J. S. Alden, A. M. van der Zande, J. M. Parpia, H. G. Craighead, and P. L. McEuen, *Nano Lett.* **8**, 2458 (2008).
15. J. S. Bunch, A. M. van der Zande, S. S. Verbridge, I. W. Frank, D. M. Tanenbaum, J. M. Parpia, H. G. Craighead, and P. L. McEuen, *Science* **315**, 490 (2007).